Laser-Induced Fluorescence of Molybdenocene and Tungstenocene in Low-Temperature Matrices

Jeremy N. Hill, Robin N. Perutz,* and A. Denise Rooney[1]

Department of Chemistry, University of York, York YO1 5DD, U.K.

Received: June 20, 1994[⊗]

The reactive metallocenes, tungstenocene and molybdenocene ($M(\eta^5\text{-}C_5H_5)_2$; M = Mo, W), have been generated by photolysis of the corresponding dihydride complexes, $M(\eta^5\text{-}C_5H_5)_2H_2$, in argon and nitrogen matrices at 12 K. The metallocenes have been probed by laser-induced fluorescence with a pulsed tunable laser and by UV/vis absorption spectroscopy. Structured emission is observed from the LMCT excited states (lifetimes < 10 ns). The spectra are complicated by multiple sites/conformers, but emission spectra of a single site/conformer may be obtained with appropriate selection of matrix and excitation wavelength. Corresponding excitation spectra are measured from the area of selected emission peaks as a function of excitation wavelength. Vibrational progressions are dominated by the ring−metal−ring symmetric stretching mode ($\nu_4 \approx 300$ cm^{-1}). Nevertheless, this mode changes in frequency by ≤ 4 cm^{-1} ($\leq 1.3\%$) in the LMCT excited state. The best-resolved peaks have a full width at half-maximum of ca. 10 cm^{-1}. Most of the emission is vibrationally fully relaxed, but weak emission peaks arising from $v' = 1$ states are found for $MoCp_2$ in N_2 matrices.

Introduction

In spite of the immense number of investigations of the photochemistry of organometallics, spectroscopic information on excited states is very restricted.[2] The power of laser-induced fluorescence (LIF) as a probe to determine excited-state and ground-state properties of matrix-isolated open-shell metallocenes was demonstrated in the preceding paper through the example of rhenocene.[3] We now use the same techniques to examine the d^4 metallocenes, molybdenocene and tungstenocene (MCp_2; M = Mo, W; Cp = η^5-C_5H_5). Both WCp_2 and $MoCp_2$ have been implicated in numerous photochemical reactions in solution.[4] Here, these two molecules are generated by photolysis of the corresponding dihydride complexes, MCp_2H_2, in argon and nitrogen matrices. They have already been the subject of extensive study by matrix isolation with detection by IR and UV/vis absorption spectroscopy and by magnetic circular dichroism (MCD).[4−7] They have a ground electron configuration $e_2{}^3a_1{}^1$, leading to a $^3E_2$ ground electronic state. In the case of WCp_2, spin−orbit coupling quenches any Jahn−Teller splitting, leading to a well-defined E_2 ($\Omega = 3$) ground spin−orbit state. An electronic IR transition to a higher spin−orbit state is prominent. For $MoCp_2$, the Jahn−Teller effect and spin−orbit coupling are of comparable magnitude, resulting in broader IR bands than for WCp_2 and no IR electronic transition. Both molecules exhibit an intense LMCT absorption band with onset at ca. 400 and 420 nm for WCp_2 and $MoCp_2$, respectively. The upper state has been demonstrated to be of E_2 symmetry by MCD. The background to the vibrational spectroscopy of metallocenes has been summarized in the preceding paper. We now report vibrationally resolved emission spectra induced by irradiation with a tunable pulsed laser. We deduce excitation spectra from the variation in the area of individual peaks of the dispersed emission spectra as a function of excitation wavelength. Some of the results presented here have been described in preliminary communications.[8,9]

Experimental Section

The experimental setup for LIF is described in detail in the preceding paper.[3] $MoCp_2H_2$ and WCp_2H_2 were synthesized by standard methods.[10] $MoCp_2H_2$ was cocondensed with matrix gas for ca. 130 min with the sample held at 310−313 K and the window at 20 K. The matrix was then cooled to 12 K before photolyzing for 60 min ($\lambda > 200$ nm). For WCp_2H_2, the sublimation temperature was 318 K and photolysis time 30 min. In each experiment, it was verified that emission intensity varied linearly with laser energy.

UV/vis and IR absorption spectra of the metallocenes were determined with a matrix apparatus which has been described elsewhere.[11] UV/vis spectra were recorded on a Perkin-Elmer Lambda 7G spectrometer (resolution 0.25 nm) and IR spectra on a Mattson/Unicam RS FTIR spectrometer (resolution 1 cm^{-1}).

Results

1. WCp_2 in Nitrogen Matrices. The formation of WCp_2 by photolysis of WCp_2H_2 in a nitrogen matrix is illustrated by the difference IR spectrum in Figure 1. The intense band at 3238 cm^{-1} is assigned as an electronic transition between spin−orbit substates, first seen in argon matrices.[5,6] The figure also shows the growth of the ring-breathing (1085 cm^{-1}) and C−H deformation (981, 971 cm^{-1} split) modes of WCp_2 and the loss of W−H modes of the precursor at ca. 1900 cm^{-1}.[12] The UV/vis absorption spectrum of WCp_2 shows the structured LMCT transition between 370 and 405 nm. The absorption spectrum before annealing shows three clear progressions in the ring−metal−ring symmetric stretching mode, ν_4', of ca. 319 cm^{-1}, arising from WCp_2 in three distinct sites/conformers labeled α, β, and γ (Figure 2a; Table I, supplementary material). However, the site structure is simplified into two dominant components, split by ca. 90 cm^{-1}, when the matrix is warmed to 30 K and subsequently recooled (Figure 2b). One component comes close to wavelengths of β site absorption, whereas the other site is quite new (δ). The separation between successive members of each progression, ν_4', is about 314 cm^{-1} (Table I, supplementary material).

The structure in this spectrum and others in this paper is labeled as follows: upper case letters refer to a progression series, "A" is the series $n\nu_4$ ($n = 0, 1, 2, \ldots$) and "B" is the combination series due to $\nu_3 + n\nu_4$; Greek superscripts symbolize a particular site/conformer; the numerals correspond to a particular overtone of the progression. For example, $A^{\alpha}3$

[⊗] Abstract published in *Advance ACS Abstracts,* November 15, 1994.

0022-3654/95/2099-0538$09.00/0

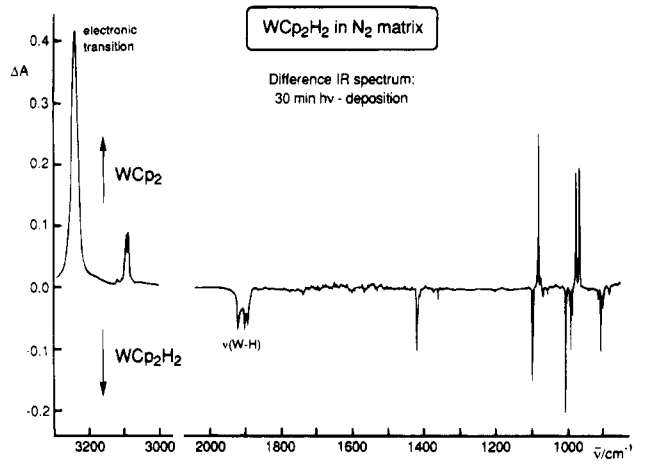

Figure 1. WCp_2H_2 in a nitrogen matrix at 12 K, after 30-min photolysis $\lambda > 200$ nm. The IR difference spectrum shows the formation of WCp_2 (positive absorbances) and depletion of the WCp_2H_2 precursor (negative absorbances).

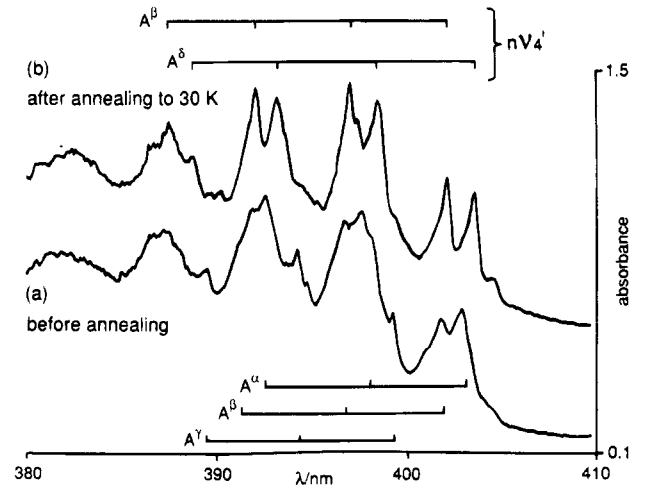

Figure 2. UV/vis absorption spectra of (a) WCp_2 obtained after deposition of WCp_2H_2 with nitrogen followed by 1-h photolysis, $\lambda > 200$ nm, and (b) WCp_2 after annealing to 30 K and recooling to 12 K. The labels A^β and A^δ refer to the annealed spectrum and indicate progressions in ν_4'.

symbolizes the third overtone ($v = 3 \leftarrow 0$) in the ν_4 progression of site/conformer α. As for rhenocene, only three vibrations are involved in the vibrational progressions. They are the totally symmetric modes, ν_4, ν_3, and ν_2, corresponding to ring−metal−ring stretching, C−H deformation and ring-breathing, respectively.[12]

Irradiation into the LMCT band of an unannealed matrix excites an intense emission spectrum (Table II, supplementary material) with a progression in ν_4'' for the three sites/conformers, α, β, and γ.[9] The (0,0) bands in *emission* for these sites/conformers are shifted between 25 and 39 cm^{-1} to lower energy than the corresponding features in the unannealed *absorption* spectrum. The relative intensity of α, β, and γ is dependent on the excitation wavelength but no component may be excited exclusively. The mean value of ν_4'' from all components is 318 cm^{-1}, very close to the value of ν_4' obtained from the absorption spectra. A value of ν_3'' of 797 cm^{-1} is measured from this spectrum (see Table II, supplementary material).

The emission spectra show dramatic changes when the matrix is annealed. Irradiation at 392.1 nm, which corresponds to the $A^\beta 2$ absorption band, induces fluorescence from the A^β site only (Figure 3a). A combination progression B ($\nu_3'' + n\nu_4''$) is easily identified, yet there is no clear peak that can be assigned to

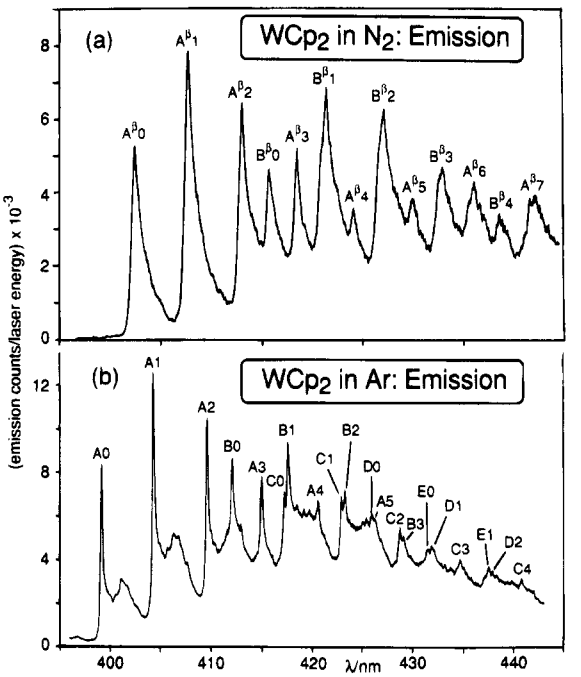

Figure 3. (a) Emission spectrum of WCp_2 in a nitrogen matrix at 12 K after annealing, $\lambda_{ex} = 392.1$ nm. (b) Emission spectrum of WCp_2 in an argon matrix at 12 K, $\lambda_{em} = 394.3$ nm.

ν_2''. No such well-resolved emission spectrum could be obtained prior to annealing with any excitation wavelength. The spectrum is comparable to that of $ReCp_2$, although the bands are much broader (fwhm = 73 cm^{-1}; cf. ca. 20 cm^{-1} for $ReCp_2$). Figure 3b shows the corresponding spectrum in an argon matrix (see below).

The changes with excitation wavelength that occur in the emission spectra of annealed samples are more subtle than encountered in the $ReCp_2$ system. Emission from the β-series is detected even if γ- or δ-series absorption bands are irradiated. Emission from the γ-series is also observed on irradiation into the γ-series absorption bands, but emission from the δ-series is very weak, even when the δ-series absorption bands are irradiated directly. These results are suggestive either of energy transfer between sites/conformers or of interconversion between sites.

It is harder to record a reliable excitation spectrum for WCp_2 than for $ReCp_2$ because the laser dyes needed to excite emission in the range 350−400 nm work less efficiently than in the range 450−500 nm. The excitation profile of the $A^\beta 1$ emission band reproduces the positions of the absorption bands of the β-site well. Despite the selectivity for the β site, the excitation spectrum offers no significant improvement in resolution compared to the annealed absorption spectrum.

The decay kinetics of the excited state show that the emission decays within the duration of the laser pulse. This result allows only an upper limit to be set on the lifetime, τ, of 10 ns.

2. WCp_2 in Argon Matrices. The LMCT absorption band of WCp_2 in an argon matrix at 12 K is slightly blue-shifted in energy compared to that in nitrogen. The vibrational band spacing is ca. 321 cm^{-1}, similar to that determined in nitrogen matrices, but the fine structure (37−75 cm^{-1}) is much less marked and shows no substantial changes when the matrix is annealed.[5] Irradiation into the LMCT absorption band leads to intense emission (Figure 3b, Table 3). The emission spectrum consists of a sharp and a broad component, separated by 120 cm^{-1}. The fundamentals ν_4'', ν_3'', and ν_2'' are measured from the A, B, and C progressions, respectively (Figure 3b).

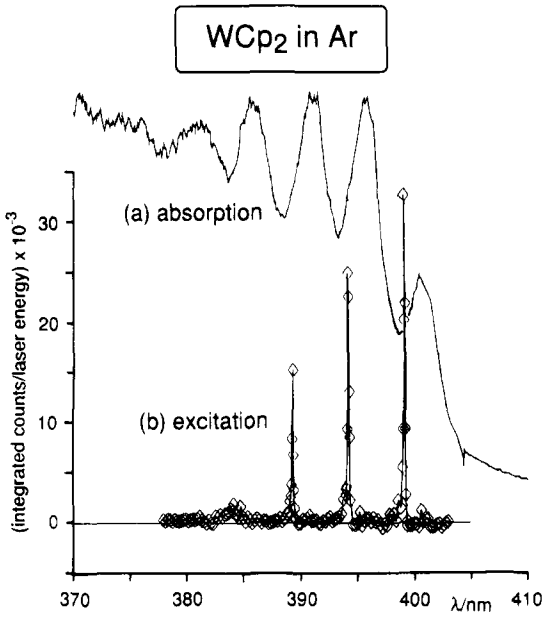

Figure 4. Spectra of WCp_2 isolated in an argon matrix at 12 K. (a) Absorption spectrum; (b) excitation spectrum determined from variation of the area of the A2 emission band with excitation wavelength.

TABLE 3: Emission Spectrum for WCp_2 in an Argon Matrix, λ_{ex} = 394.3 nm (See Figure 3b)

λ, nm	$\bar{\nu}$, cm^{-1}	$\Delta\bar{\nu}$, cm^{-1} (from origin)	label	assgt	interval, cm^{-1}
399.16	25 053	0	A0	T_0	0
404.31	24 734	319	A1	ν_4''	A0 − 319
409.64	24 412	641	A2	$2\nu_4''$	A1 − 322
412.16	24 262	791	B0	ν_3''	T_0 − 791
415.04	24 094	959	A3	$3\nu_4''$	A2 − 318
417.28	23 965	1088	C0	ν_2''	T_0 − 1088
417.68	23 942	1111	B1	$\nu_3'' + \nu_4''$	B0 − 320
420.6	23 774	1279	A4	$4\nu_4''$	A3 − 320
423.0	23 643	1410	C1	$\nu_2'' + \nu_4''$	C0 − 322
423.3	23 624	1429	B2	$\nu_3'' + 2\nu_4''$	B1 − 318
426.0	23 473	1580	D0	$2\nu_3''$	B0 − 789
426.4	23 455	1598	A5	$5\nu_4''$	A4 − 319
428.8	23 323	1730	C2	$\nu_2'' + 2\nu_4''$	C1 − 320
429.1	23 303	1750	B3	$\nu_3'' + 3\nu_4''$	B2 − 321
431.5	23 175	1878	E0	?	T_0 − 1878
431.9	23 156	1897	D1	$2\nu_3'' + \nu_4''$	D0 − 317
434.7	23 004	2049	C3	$\nu_2'' + 3\nu_4''$	C2 − 319
437.6	22 854	2199	E1	?	E0 − 321
437.9	22 835	2218	D2	$2\nu_3'' + 2\nu_4''$	D1 − 321
440.8	22 686	2367	C4	$\nu_2'' + 4\nu_4''$	C3 − 318

An excitation profile of the A2 band area is shown as Figure 4b (Table 4). Compared to the absorption spectrum (Figure 4a), the excitation profile is much more highly resolved with a clear progression in ν_4'. The (0,0) band positions in excitation and emission are coincident. However, the intensity profile of the excitation maxima does not resemble the intensity profile of the absorption and emission spectra: there is no clear ν_3' band and the emission intensity decreases monotonically with vibrational quantum number. The A3 emission intensity is very low relative to A2, whereas the A3 absorption intensity is still high.

Expansions of the A1 transition show that the excitation band is narrower (fwhm ≈ 10 cm^{-1}, Figure 5a) than the equivalent band in the emission spectrum (fwhm = 17 cm^{-1}, Figure 5b). The broad component of the emission spectrum is conspicuous in emission but is not seen in excitation, as it has been effectively subtracted out. Both excitation and emission bands are more symmetric than those seen in for $ReCp_2$.

TABLE 4: Excitation Spectrum of the A2 Emission Band of WCp_2 in Argon Matrices (See Figure 4b)

λ, nm	$\bar{\nu}$, cm^{-1}	$\Delta\bar{\nu}$, cm^{-1} (from origin)	label	assgt	interval, cm^{-1}
399.15	25 053	0	A0	T_0	0
394.20	25 368	315	A1	ν_4'	A0 + 315
389.35	25 684	631	A2	$2\nu_4'$	A1 + 316
384.8	25 988	935	A3	$3\nu_4'$	A2 + 305
384.2	26 028	975	?	?	?

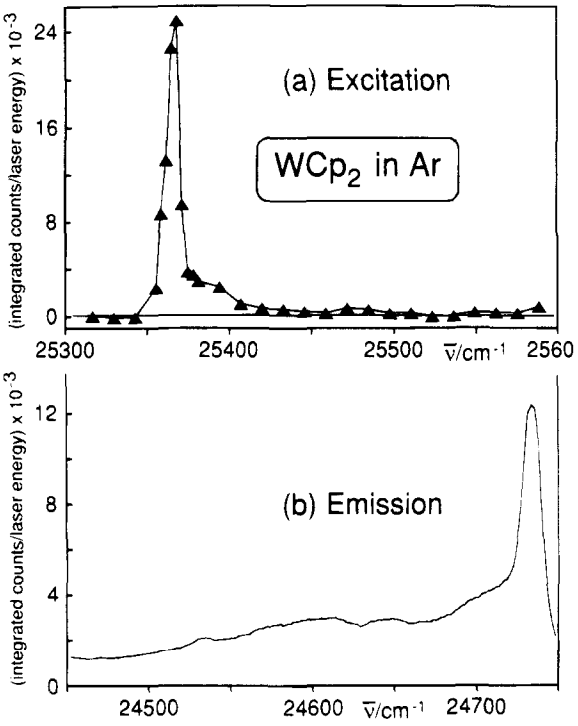

Figure 5. (a) Expanded *excitation* spectrum of WCp_2 in an argon matrix showing the A1 (1 ← 0) band only. (b) Expanded *emission* spectrum of WCp_2 in an argon matrix at 12 K, showing just the A1 (0 → 1) transition (λ_{ex} = 399.15 nm).

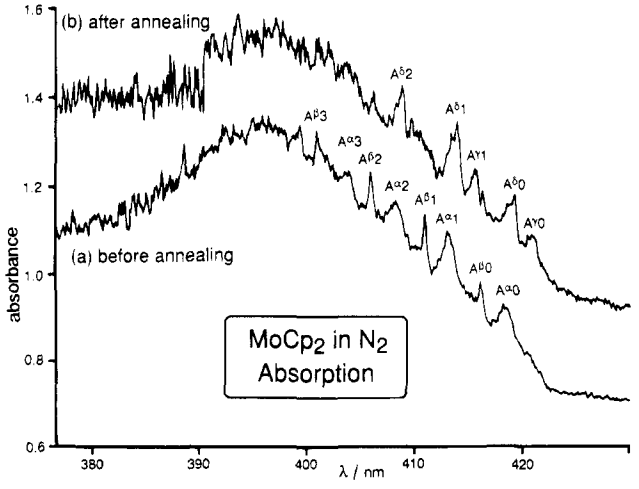

Figure 6. UV/vis *absorption* spectrum for $MoCp_2$ in a nitrogen matrix at 12 K: (a) before annealing, (b) after annealing to 30 K and recooling.

3. $MoCp_2$ in Nitrogen Matrices. The LMCT transition of $MoCp_2$ in a nitrogen matrix has its onset ca. 16 nm to longer wavelength than that of WCp_2. The absorption band is also appreciably broader than that of the tungsten analogue (Figure 6; Table V, supplementary material). Prior to annealing, the absorption spectrum contains two progressions, A^{α} and A^{β}, separated by ca. 140 cm^{-1} (Figure 6a). The interval between successive members of each progression is about 300 cm^{-1} and

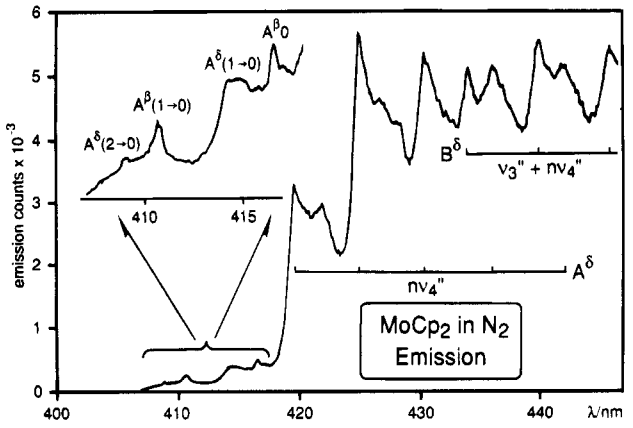

Figure 7. *Emission* spectrum of $MoCp_2$ in a nitrogen matrix at 12 K after annealing to 30 K and recooling (λ_{ex} = 402.0 nm). The inset shows an expansion of the short-wavelength region including unrelaxed emission.

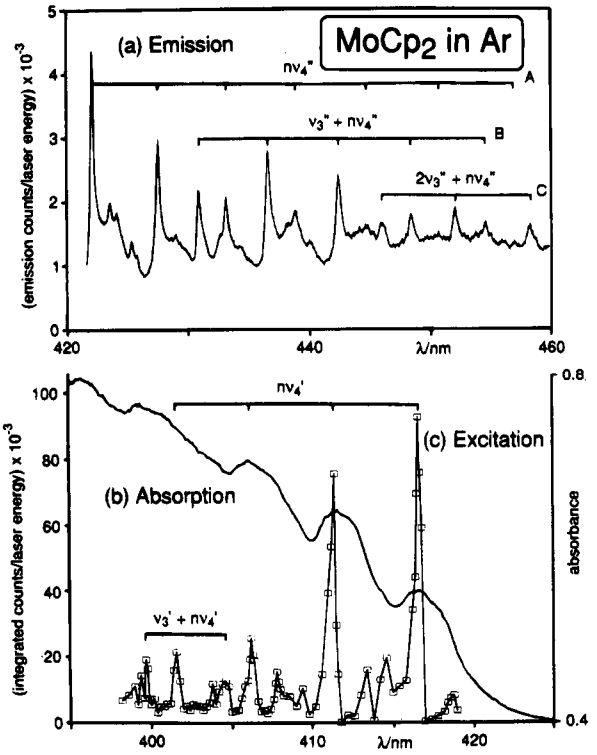

Figure 8. (a) *Emission* spectrum of $MoCp_2$ in an argon matrix at 12 K. (b) UV/vis absorption spectrum of $MoCp_2$. (c) *Excitation* spectrum determined from the variation of the area of the A2 emission band with excitation wavelength.

corresponds to ν_4'. When the matrix is annealed (Figure 6b) two different series, A^γ and A^δ, are seen. Each series appears to be superimposed upon a much broader, unstructured band.

Irradiation into the LMCT band produces relatively poorly resolved fluorescence spectra regardless of whether the matrix has been annealed (Figure 7; Table VI, supplementary material). The emission spectrum shows the ν_4'' progression and the combination series due to $\nu_3'' + n\nu_4''$. The onset of the main emission is at 419.5 nm, close to the position of the $A^\delta 1$ absorption band. Multiple components are identified when the excitation wavelength is changed, but the large proportion of unstructured emission remains.

The weak emission bands appearing at *shorter* wavelengths than the assigned electronic origin $A^\delta 0$ are enlarged in the inset of Figure 7. The longest wavelength of these bands arises from fully relaxed fluorescence: $A^\beta 0$ ($\lambda_{em} \approx 416.1$ nm). The other features are observed at shorter wavelengths, suggesting that they originate from unrelaxed emission. The proposed transitions are given on Figure 7.

TABLE 7: Principal Features of the *Emission* Spectrum of $MoCp_2$ in an Argon Matrix, λ_{ex} = 416.6 nm (See Figure 8a)

λ, nm	$\bar{\nu}$, cm^{-1}	$\Delta\bar{\nu}$, cm^{-1} (from origin)	label	assgt	interval, cm^{-1}
416.6[a]	*24 004*	*0*	*A0*	*T_0*	*0*
422.1	23 691	313	A1	ν_4''	$T_0 - 313$
427.6	23 386	618	A2	$2\nu_4''$	A1 − 305
430.9	23 207	797	B0	ν_3''	$T_0 - 797$
433.2	23 084	920	A3	$3\nu_4''$	A2 − 302
436.6	22 904	1100	B1	$\nu_3'' + \nu_4''$	B0 − 303
438.9	22 784	1220	A4	$4\nu_4''$	A3 − 300
442.5	22 599	1405	B2	$\nu_3'' + 2\nu_4''$	B1 − 305
444.7	22 487	1517	A5	$5\nu_4''$	A4 − 297
446.0	22 422	1582	D0	$2\nu_3''$	B0 − 785
448.5	22 297	1707	B3	$\nu_3'' + 3\nu_4''$	B2 − 302
450.7	22 188	1816	A6	$6\nu_4''$	A5 − 299
452.1	22 119	1885	D1	$2\nu_3'' + \nu_4''$	C0 − 303
454.7	21 993	2011	B4	$\nu_3'' + 4\nu_4''$	B3 − 304
457.1	21 877	2127	A7	$7\nu_4''$	A6 − 311
458.4	21 815	2189	D2	$2\nu_3'' + 2\nu_4''$	C1 − 304

[a] Position of the (0,0) is taken from the excitation spectrum.

TABLE 8: *Excitation* Spectrum of $MoCp_2$ in an Argon Matrix (See Figure 8c)

λ, nm	$\bar{\nu}$, cm^{-1}	$\Delta\bar{\nu}$, cm^{-1} (from origin)	label	assgt	interval, cm^{-1}
416.6	24 004	0	A0	T_0	0
411.4	24 307	303	A1	ν_4'	$T_0 + 303$
406.2	24 618	614	A2	$2\nu_4'$	A1 + 311
404.4	24 728	724	B0	ν_3'	$T_0 + 724$
401.2	24 925	921	A3	$3\nu_4'$	A2 + 307
399.7	25 019	1015	B1	$\nu_3' + \nu_4'$	B0 + 291

Lifetime measurements of the excited state were attempted, but the duration of the laser pulse again exceeds the emission lifetime, allowing only an upper limit to be set at 10 ns.

4. $MoCp_2$ in Argon Matrices. The absorption spectrum of $MoCp_2$ in an argon matrix[5] is similar in appearance to that in a nitrogen matrix, although the site structure is less distinct. The best-resolved emission spectra are obtained when exciting into the (0,0) transition of the absorption spectrum (Figure 8a, Table 7). (Note that this figure does not show the (0,0) emission band since it is close to the laser line.) Progression series, $n\nu_4''$ (A), $\nu_3'' + n\nu_4''$ (B), and $2\nu_3'' + n\nu_4''$ (C) are observed. Site structure is apparent in all the spectra recorded, and different features appear to be probed selectively according to the laser wavelength. More congested spectra are obtained when shorter wavelength excitation is used. The spectra all show a substantial unstructured, background fluorescence. Shorter wavelength excitation induces some emission at shorter wavelengths than the (0,0) band, akin to that seen in a nitrogen matrix.

An excitation spectrum may be obtained by recording the area of the A2 emission band as a function of laser wavelength and energy (Figure 8c, Table 8). The excitation profile shows a dramatic improvement in resolution when compared to the absorption spectrum (Figure 8b), allowing values for the excited-state vibrations ν_4' and ν_3' to be obtained. Notice that the excitation spectrum gives the impression that short-wavelength excitation does not induce emission. In fact, substantial fluorescence is observed, but it is poorly resolved and the area of the A2 band cannot be measured reliably.

The lifetime of the excited state proved shorter than the duration of the laser pulse (i.e., <10 ns).

Discussion

The d^4 metallocenes, WCp_2 and $MoCp_2$, exhibit intense structured emission from their LMCT excited states. The LIF

TABLE 9: Progression Frequencies ($\bar{\nu}$, cm^{-1}) of Metallocenes in the Ground and Excited States with the Estimated Standard Error (95% Probability), Where Available, in Parentheses

compound	matrix/phase	ν_4''	ν_4'	ν_3''	ν_3'	ν_2''	ν_2'
$ReCp_2$	Ar	323 (7)	340 (4)	818	745	1097	1060
	N_2	325 (5)	342 (3)	826	754	1100	1063
WCp_2	Ar	320 (3)	316	790		1088	
	N_2[a]	318 (6)	316 (12)	797			
	N_2[b]	318 (11)	313 (24)	789			
$MoCp_2$	Ar	303 (7)	307	791	724		
	N_2	300 (21)	302 (12)	791			
$RuCp_2$[c]	crystal	333	279			1104	
ZnCp[d]	gas	254	279	772	737	1001	953

[a] Prior to annealing. [b] After annealing. [c] From ref 14. [d] From ref 13.

spectra have many features in common with the spectra of $ReCp_2$. The emission occurs from the same state as that probed by the laser, with (0,0) bands close to coincidence in emission, absorption, and excitation. The vibrational progression in the ring−metal−ring symmetric stretching mode, $n\nu_4$, dominates the spectrum, with weaker progressions from $\nu_3 + n\nu_4$ and sometimes, $\nu_2 + n\nu_4$ or $2\nu_3 + n\nu_4$. The spectra of WCp_2 and $MoCp_2$ are complicated by the presence of multiple trapping sites and/or conformers. By judicious choice of conditions, it is possible to obtain emission and excitation spectra dominated by a single site/conformer. Some of the excitation spectra are much sharper than the corresponding absorption spectra.

There are also several features of the spectra which differ significantly from those of $ReCp_2$, some of which are described in more detail below: (i) the emission lifetimes are all too short to measure with the current apparatus (<10 ns, compared with 72 ns for $ReCp_2$); (ii) the differences between ground- and excited-state values of ν_4 are very small ($\leq$4 cm^{-1}); (iii) the narrowest emission and excitation bands of $MoCp_2$ and WCp_2 (in argon matrices) are close to symmetrical, unlike the skew shape observed for $ReCp_2$; (iv) the intensity profiles of the emission and excitation spectra, especially of WCp_2 in Ar, are not mirror images; (v) the spectra of $MoCp_2$ show evidence for unrelaxed emission.

1. Vibrational Fine Structure. The totally symmetric vibrational frequencies determined from the LIF spectra are listed in Table 9 together with values for other metallocenes. Although the spectra of $MoCp_2$ and WCp_2 are dominated by progressions in ν_4, the differences between ground- and excited-state values of ν_4 are so small ($\leq$4 cm^{-1}) as to be insignificant when errors are taken into account. It proved possible to determine ν_3'' in all emission spectra, but the corresponding value of ν_3' was determined only for $MoCp_2$ in argon matrices. In that case, a reduction of 67 cm^{-1} (8.4%) was found. Only one value of ν_2'' was measured and none of ν_2'. Since ν_4 is the progression-forming mode, there must be a change in the metal−ring bond length in the excited state. The lack of a corresponding change in ν_4 indicates that ν_4 does not correlate simply with bond length and that there must also be changes in coupling between vibrations in the excited state.

The symmetric band shape with fwhm of 10−20 cm^{-1} found in the sharpest spectra of WCp_2 in solid argon implies that there is no coupling either to matrix phonons or torsional overtones as postulated to explain the skew shape of rhenocene bands.

It is valuable to compare the changes in the frequencies between ground and excited states for the range of metallocenes (Table 9). The transition involved in the cases of $ReCp_2$, $MoCp_2$, and WCp_2 transfers an electron from a ligand π-orbital to a metal−ligand bonding orbital. For $ReCp_2$ this results in an increase in ν_4, but for the d^4 metallocenes, there is essentially no change. For $ReCp_2$ there is also a substantial fall in ν_3 and ν_2. The data for the d^4 metallocenes are incomplete, only allowing us to state that there is a similar reduction in ν_3 for $MoCp_2$. The transition involved in emission from ZnCp also has LMCT character,[13] though this time the electron is transferred to a metal p-orbital. The changes in frequency are remarkably similar to those found for $ReCp_2$ in spite of the drastic difference in electron configuration and the reduced value of ν_4. In contrast, the emission from crystalline $RuCp_2$ arises from a spin-forbidden ligand-field band,[14] so the electron is transferred to an orbital which is strongly metal−ligand antibonding. As a result, the value of ν_4 falls by 54 cm^{-1} (16%). The relation between the changes in the frequency and the changes in geometry will be developed in a subsequent paper via Franck−Condon analysis.

2. Unrelaxed Emission. The emission spectra of $MoCp_2$ in nitrogen matrices show weak features to high energy of the electronic origin with frequencies which fit with emission from $v' = 1$ levels. This observation is consistent with a very short emission lifetime and a comparable relaxation time. The broadening of emission spectra when higher vibrational quanta are probed may be another manifestation of unrelaxed emission, since it would give rise to multiple overlapping bands. It may also contribute to the broadening of the high-energy features of the excitation spectra (e.g., Figure 4) so the excitation profile does not mirror the emission profile. For comparison, unrelaxed emission is much more important in the gas phase, as has been observed for ZnCp.[13]

Conclusions

The d^4 metallocenes $MoCp_2$ and WCp_2 isolated in N_2 and Ar matrices exhibit well-resolved fluorescence spectra when excited with a pulsed tunable laser. Both absorption and emission involve the same fully allowed LMCT excited state with lifetime <10 ns. The spectra are complicated by the presence of multiple sites/conformers, but emission spectra of a single site can be obtained with suitable choice of matrix and excitation wavelength. Similarly, single-site excitation spectra can be obtained with suitable choice of emission maximum. The spectra are dominated by progression series in the symmetric ring−metal−ring stretching mode, $n\nu_4$, with additional progressions in $\nu_3 + n\nu_4$, $\nu_2 + n\nu_4$, and $2\nu_3 + n\nu_4$. Nevertheless, the changes in ν_4 between ground and excited states are $\leq$4 cm^{-1} ($\leq$1.3%), implying that the vibrational frequencies do not correlate well with the geometric coordinate.

Acknowledgment. We are particularly grateful to Dr. A. W. Parker and S. Tavender of the Rutherford-Appleton Laboratory for their support. We also appreciate the help given by Dr. S. E. J. Bell, S. A. Brough, and Dr. A. McCamley. We thank Prof. M. L. H. Green for a sample of WCp_2H_2. This work was supported by SERC, The Royal Society, British Gas and the European Commission.

Supplementary Material Available: Tables I, II, V, VI: UV/vis absorption and emission spectra for WCp_2 and $MoCp_2$ in nitrogen matrices (5 pages). Ordering information appears on any current masthead page.

References and Notes

(1) Present address: Department of Chemistry, St. Patrick's College, Maynooth, Ireland.

(2) *Photoprocesses in Transition Metal Complexes, Biosystems and other Molecules. Experiment and Theory*; Kochanski, E., Ed.; NATO ASI Series C; Kluwer Academic Publishers: Dordrecht, 1992; Vol. 376. Turner, J. J.; Johnson, F. P. A.; Westwell, J. R. *Coord. Chem. Rev.* **1993**, *125*, 101.

(3) Hill, J. N.; Perutz, R. N.; Rooney, A. D. Preceding paper in this issue.

(4) Grebenik, P.; Grinter, R.; Perutz, R. N. *Chem. Soc. Rev.* **1988**, *17*, 453.
(5) Chetwynd-Talbot, J.; Grebenik, P.; Perutz, R. N. *Inorg. Chem.* **1982**, *21*, 3647.
(6) Cox, P. A.; Grebenik, P.; Perutz, R. N.; Robinson, M. D.; Grinter, R.; Stern, D. R. *Inorg. Chem.* **1983**, *22*, 3614.
(7) Graham, R. G.; Grinter, R.; Perutz, R. N. *J. Am. Chem. Soc.* **1988**, *110*, 7036.
(8) Bell, S. E. J.; Hill, J. N.; McCamley, A.; Perutz, R. N. *J. Phys. Chem.* **1990**, *94*, 3876.
(9) Perutz, R. N.; Hill, J. N.; McCamley, A. *Coord. Chem. Rev.* **1991**, *111*, 111.
(10) Green, M. L. H.; Knowles, P. J. *J. Chem. Soc., Perkin Trans. 1* **1973**, 989.
(11) Haddleton, D. M.; McCamley, A.; Perutz, R. N. *J. Am. Chem. Soc.* **1988**, *110*, 1810.
(12) Aleksanyan, V. T. In *Vibrational Spectra and Structure*; Durig, J. R., Ed.; Elsevier: Amsterdam, 1982; Vol. 11.
(13) Robles, E. S. J.; Ellis, A. M.; Miller, T. A. *J. Phys. Chem.* **1992**, *96*, 3247.
(14) Riesen, H.; Krausz, E.; Luginbühl, W.; Biner, M.; Güdel, H. U.; Ludi, A. *J. Chem. Phys.* **1992**, *96*, 4131. Wrighton, M. S.; Pdungsap, L.; Morse, D. L. *J. Phys. Chem.* **1975**, *79*, 66. Hollingsworth, G. J.; Kim Shin, K.-S.; Zink, J. I. *Inorg. Chem.* **1990**, *29*, 2501.